Journal of Medical Phyto Research
Vol. 2, Article 3, (27-34)

ISSN: 2577-6541
Doi: 10.31013/2001g

Bioactive cannabidiol more greatly reduces valvular interstitial cell calcification when combined with ß-Caryophyllene, and α-Humulene

D. Cushing[1]*, D. Goakar[2], & B. Joseph[1,2]

[1]: Peak Health Center, Los Gatos, CA

[2]: ImmunAG LLP, Goa, India

*For inquiries, email corresponding author at donish@peakhealth.center

Abstract:

Valvular interstitial cells (VICs) are integral to heart valve homeostasis and structural leaflet integrity. Aberrant calcification of VICs leads to dangerous diseases including calcific aortic valve disease. VIC calcification can be reduced by cannabidiol (CBD) through modulation of the ERK cascade by selective antagonism of the CB2 receptor, and possible involvement of the GPR55 receptor. ß-Caryophyllene (BCP) and α-Humulene (HMU) are sequiterpenes that produce their own effects on calcification. The present study aimed to see whether a combination of CBD, BCP, and HMU (ImmunAG) could reduce calcification to a greater extent than CBD alone. VICs were isolated from porcine aortic valve leaflets, induced to calcify, and treated with CBD or ImmunAG. Treatment concentrations of 5, 10, 25, 40, and 100 mg were examined. Means, standard deviations, minimum, and maximum calcification reduction values for each treatment and mg concentration are provided. 5 *t*-tests revealed that ImmunAG reduced calcification more than CBD at every concentration.

Within the complex multichambered pump that is the human heart exist supple, flow-regulating membranes known as heart valves (Mohler et al., 2001; Butcher, Simmons, & Warnock, 2008). Within these valves, among an extracellular matrix, exist valvular interstitial cells (VICs), which are integral to valve homeostasis and structural leaflet integrity (Hjortnaes et al., 2015; Taylor, Batten, Brand, Thomas, & Yacoub, 2003).

Calcium salts can be abnormally deposited among soft tissues, causing them to harden and reducing their capacity to function properly. Calcification of VICs causes disruption of interstitial cell mechanical phenotype, and drives interstitial matrix disorganization, nodule formation, and pro-calcific signaling (Farrar, Pramil, Richards, Mosher, & Butcher, 2016). This can lead to any number of dystrophic calcification diseases of the heart that each can increase the risk for developing other cardiovascular diseases (e.g., valvular stenosis, see Michel & Dipchand, 2017; de Simone et al., 2010; Gerdts et al., 2015).

A previous study by Cushing, Goakar, and Joseph (2018), showed that cannabidiol (CBD) extracted from Kriya Brand Humulus significantly reduced VIC calcification. Higher bioactivity CBD caused greater reductions. The highest bioactivity CBD (bioactivity = .95) at the highest concentration (100mg) caused a mean reduction of 55% (*SD* = 6.66). While this is certainly noteworthy, the addition of other synergistic phyo-compounds may reduce calcification further.

β-Caryophyllene (BCP) is a natural bicyclic sesquiterpene abundantly found in essential oils from various spices, fruits and plants. It is approved by United States Food and Drug Administration and European agencies as food additive, taste enhancer and flavoring agent and considered a dietary phytocannabinoid (Sharma, M Al Kaabi, Nurulain, Goyal, Amjad Kamal, & Ojha, 2016). BCP has anti-inflammatory, antibiotic, antioxidant, anticarcinogenic and local anaesthetic properties (Legault & Pichette, 2007). It is a functional selective agonist for the CB_2 receptor (Sharma et al., 2016; Bahi, Al Mansouri, Al Memari, Al Ameri, Nurulain, & Ojha, 2014; Gertsch et al., 2008), which attenuates ERK activity (Gu & Masters, 2009), and the peroxisome-proliferator activating receptor alpha (PPARα; Poddighe et al., 2018), which exerts anti-inflammatory effects in the vascular wall (Zandbergen & Plutzky, 2007).

α-Humulene (HMU) is an isomer of BCP. HMU is generally not studied in isolation. It has no affinity for CB_2. It exerts anti-calcific effects indirectly, through reduction of inflammation. It can prevent the production of pro-inflammatory cytokines by suppressing NF-kB activation in macrophages (Yoon et al., 2010).

BCP and HMU can be extracted from Kriya Brand Humulus without adversely affecting the bioactivity of the CBD. The present article examines the effects that a proprietary blend of high bioactivity CBD, BCP, and HMU, called ImmunAG, has on VIC calcification compared to high bioactivity CBD alone.

Results:

Multiplate wells containing calcifying VICs from 27 different tissue samples were treated with 5, 10, 25, 40, or 100mg of either CBD or ImmunAG. Average calcification was computed using the number of nodules per well, and the average area per nodule. Mean nodule area for untreated wells was 3.27 mm^2 (*SD* = 0.32, *min* = 0.5, *max* = 4.0) per well. All reported percent reductions in calcification were computed by dividing average nodule area of treated wells from 3.27 mm^2.

Means, standard deviations, and minimum and maximum values for CBD and ImmunAG for every tested mg concentration are provided in Table 1. (Full data are provided in the Appendix.) Paired-samples *t*-tests determined that ImmunAG reduced calcification significantly more than CBD alone at every mg concentration: At 5mg, $t(26) = 9.87$, $p < .001$, $d = 1.90$; at 10 mg, $t(26) = 4.20$, $p < .001$, $d = 0.81$; at 25 mg, $t(26) = 5.23$, $p < .001$, $d = 1.00$; at 40 mg, $t(26) = 7.76$, $p < .001$, d

mg		**CBD**	**ImmunAG**
5	*M*	19.42	24.32
	SD	1.8	1.77
	Min	15.4	20.1
	Max	22.1	27.8
10	*M*	25.56	30.39
	SD	3.04	4.97
	Min	18.5	19
	Max	32.5	39.7
25	*M*	32.69	38.53
	SD	4.33	4.44
	Min	26.3	26.9
	Max	42.6	46.1
40	*M*	42.98	52.83
	SD	4.8	3.65
	Min	35.8	44.6
	Max	54.5	60
100	*M*	55	64.21
	SD	6.66	7.91
	Min	41.9	51.3
	Max	66.1	78.1

Table 1: Descriptive statisticis of calcification reduction data of CBD and ImmunAG by mg concentration,

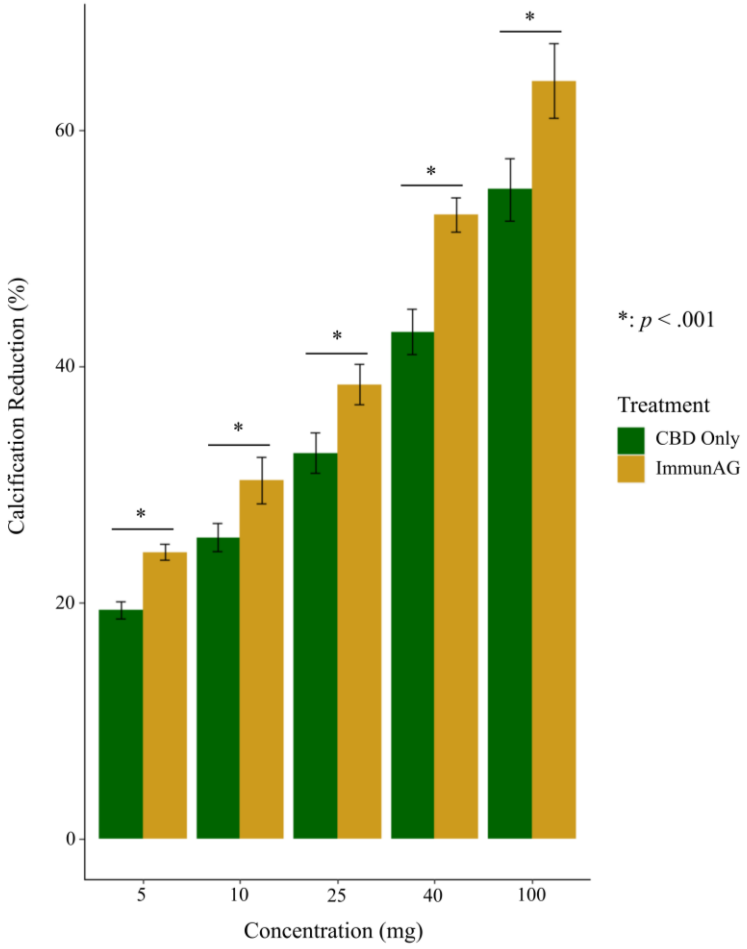

Figure 1: ImmunAG reduced calcification significantly more than CBD at every mg concentration.

= 1.49; and at 100 mg, $t(26) = 4.05$, $p < .001$, $d = 0.78$. A barplot of observed differences is given in Figure 1.

Conclusion:

This study demonstrated that a combination of high bioactivity CBD, BCP, and HMU reduced VIC calcification more than high bioactivity CBD alone. It remains to be seen whether possible synergistic effects afforded by this combination of compounds extends beyond VIC calcification. CBD has been shown to have anxiolytic, antidepressant, antipsychotic, anticonvulsant, anti-nausea, antioxidant, antiinflammatory, anti-arthritic, and anti-neoplastic properties (Ligresti Petrocellis, & Di Marzo, 2016). BCP has shown promising for anti-endemic, anti-tumoral, anti-oxidant, anti-microbial, and anti-inflammatory properties (Dahham et al., 2015). As phytoceutical approaches to medicine continue to gain traction, a uncovering the ways that each of these properties interact will constitute an exciting new frontier for science.

Method:

This study was carried out concurrently with the study described in Cushing, Goakar, & Joseph (2018). All chemicals and solutions were obtained from Sigma-Aldrich (St. Louis, MO). All cell cultures were obtained from Creative Bioarray, Shirley, NY. CBD bioactivity was measured using practices described in Cushing, Kristipati, Shastri, and Joseph (2018).

VIC isolation and culture

VICs were isolated from porcine aortic valve leaflets (Hormel, Austin, MN) by collagenase digestion and subsequently cultured in growth medium (15% FBS, 2 mML-glutamine, 100 U/ml penicillin, and 100 g/ml streptomycin in medium 199) at 37°C, 5% CO2 for two to four passages. VICs used in all experiments were seeded at a density of 50,000 cells/cm^2 onto 24-well or 96-well plates. During the experiments, the VICs were cultured in low-serum medium (1% FBS, 100 U/ml penicillin, 100 g/ml streptomycin, 2 mM L-glutamine, in medium 199), and the medium was changed each day until the fifth day.

Culture substrate coatings

Tissue culture polystyrene (TCPS) plates (24-well or 96-well) were coated with type I collagen (Coll) (Inamed Biomaterials, Fremont, CA; 2 g/cm2), fibronectin (FN, 5 g/cm2), fibrin (FB, 1.5 g/cm2), or left untreated (TCPS). For the FB coating, plates were first incubated overnight at 4°C in fibrinogen (1 mg/ml), followed by three washes with 0.05% Tween 20 in phosphate- buffered saline (PBS) and 1 h incubation with thrombin (0.6 mg/ml) at 37°C (12). All coatings were prepared in 50 mM bicarbonate coating buffer, pH 8.5, and rinsed three times with PBS before cell seeding. The amounts of adsorbed proteins were measured on separate plates using the bicinchoninic acid protein assay (Pierce, Rockford, IL) to verify adsorption of protein coatings.

MEK-1/2 inhibition

VICs exposed to various concentrations and bioactivities of CBD were treated with U-0126 [1,4-diamino- 2,3-dicyano-1,4-bis(2- aminophenylthio) butadiene; Calbiochem, San Diego, CA], PD-98059 (2-amino-3 methoxyflavone; 5 M; Calbiochem), or left untreated as a control to confirm the MAPK specificity of these inhibition experiments. U-0126 specifically inhibits MEK-1/2, thus inhibiting activation of ERK-1/2 (Favata et al., 1998). PD-98059 is an alternate MEK inhibitor (Citation). 9 tissue samples were in each treatment group. These were the tissue samples used in subsequent analyses.

Quantification of cell number

At time points of 1, 3, and 5 days, VICs were lysed with radioimmunoprecipitation assay buffer [1% sodium deoxycholate, 0.1% SDS, 1% Triton X-100, 1 mM iodoacetamide, 140 mM NaCl, 10 mM Tris HCl, (pH 8.0)]. The amount of DNA in sample lysates was measured via the Quanti-iT PicoGreen assay (Invitrogen, Carlsbad, CA), according to the manufacturer's instructions.

Migration assay

Migration was assayed via a modified fence method (Mann & West, 2002), wherein VICs were seeded within 2 mm^2 removable silicone wells, grown to confluency, and then allowed to migrate following the detachment of silicone isolators (defined as day 0). Grid-patterned transparencies were attached underneath plates containing VIC cultures to track cell movement over time. Photomicrographs were taken of the leading edge of cell migration under 40 magnification (Olympus IX51) every 24 h for 5 days. Net cell edge displacement was measured

by overlaying time course images and then quantifying migration distance (NIH ImageJ) by measuring the advancement of the leading cell edge subtracted from the migration area recorded on day 0 within a single grid space.

Apoptosis assay

To ensure the health of the cell samples used in the calcification experiment, apoptosis was measured using an ELISA-based HT TiterTACS Assay Kit (Trevigen, Gaithersburg, MD), which detects DNA fragmentation. At days 1 and 5, cells were fixed in 3.7% buffered formaldehyde solution for 7 min, washed with PBS, and postfixed in 100% methanol for 20 min. Following manufacturer's instructions, the cells were permeabilized with proteinase K, quenched with 2.5% H2O2 in methanol, and then incubated with the labeling reaction mix (TdT, Biotin-dNTP, unlabeled dNTP) to label breaks in DNA. Streptavidin-HRP and then TACS-Sapphire were added to the wells to detect apoptotic cells; the reaction was stopped with 2 N HCl, and absorbance was read at 450 nm.

RNA isolation

Total RNA was isolated using TRI Reagent (Molecular Research Center, Cincinnati, OH), according to the manufacturer's instructions. VICs were lysed with 200 l TRI Reagent per well at 4°C with 50 protease inhibitor cocktail (BD Biosciences, San Jose, CA). The homogenate was stored at room temperature for 5 min to complete the dissociation of nucleoprotein complexes, at which point 0.15 ml chloroform per 600 l TRI Reagent was added to the homogenate, followed by centrifugation at 13,000 g for 15 min. After centrifugation, RNA was precipitated from the upper aqueous phase by adding 0.3 ml isopropanol per 600 l TRI Reagent to the tubes and then centrifuged at 13,000 g for 8 min. After this centrifugation step, the RNA pellet was washed with 75% ethanol and centrifuged at 8,000 g for 5 min. The RNA pellet was air dried and dissolved in 75l H2O at 60°C for 15 min. RNA samples were stored at 20°C until subsequent use.

Quantitative real-time PCR analysis

Custom primers for various markers of cell contractility and osteogenic activity were obtained from Invitrogen (Carlsbad, CA) and are listed in Table 1. For cDNA construction, 250 ng of original RNA isolated from samples were reverse transcribed using iScript (Bio-Rad Laboratories, Hercules, CA) as per manufacturer's instructions. Samples were processed for real-time PCR analysis by combining 0.5 l of the cDNA construction, 5 M of primers, and SYBR Green SuperMix (Bio-Rad) in a 15-l reaction, as specified in the manufacturer's protocol. For thermo cycling, a standard protocol was used: PCR reactions were run over 40 cycles of denaturing at 95°C for 15 s and annealed at 60°C for 1 min; this was followed by a melting curve analysis for 80 cycles of 55°C 0.5°C/cycle, 10 s per cycle, to further confirm the purity of the final PCR products, with each condition performed in triplicate (iCycler iQ Real-Time PCR Instrument, Bio-Rad). A standard comparative threshold cycle (or CT) method was used to analyze the PCR data. The CT of all samples were first normalized to -actin as an internal control, and then the CT values for experimental samples were further normalized to the negative control (VICs on Coll, which represented a non CBD condition).

Quantification of nodule number and size

After 5 days of culture in the presence or absence of U-0126 or PD-98059, VIC cultures were stained with Alizarin Red S (ARS) to facilitate quantification of calcified nodules, as ARS stains mineralized deposits red. Cultures were fixed with 10% neutral buffered formalin, stored at 4°C overnight, and stained with a 2% solution of ARS in PBS. Positively stained nodules were manually counted under a microscope (Olympus IX51 with Hamamatsu 285 digital camera and Simple PCI digital imaging software; Compix, Imaging Systems, Cranberry Township, PA). Nodule size was measured using ImageJ software (National Institutes of Health; http://rsb.info.nih.gov/ij/), and photomicrographs were captured under 40 and 100 magnifications.

CBD and ImmunAG samples

.95 bioactivity CBD was isolated by HPLC from ImmunAG, a humulus product of ImmunAG LLP. ImmunAG is a proprietary combination of CBD (39.5%), BCP (59.5%), and HMU(1%). The bioactivity of the BCP and HMU were not directly tested. They were likely approximately equal to the bioactivity of the CBD.

References:

Bahi, A., Al Mansouri, S., Al Memari, E., Al Ameri, M., Nurulain, S. M., & Ojha, S. (2014). β-Caryophyllene, a CB2 receptor agonist produces multiple behavioral changes relevant to anxiety and depression in mice. *Physiology & behavior*, *135*, 119-124. https://doi.org/10.1016/j.physbeh.2014.06.003

Butcher, J. T., Simmons, C. A., & Warnock, J. N. (2008). Mechanobiology of the aortic heart valve. *Journal of Heart Valve Disease*, *17*(1), 62. https://doi.org/10.1007/978-1-4939-5617-3_12

Cheng, Y., Dong, Z., & Liu, S. (2014). β-Caryophyllene ameliorates the Alzheimer-like phenotype in APP/PS1 Mice through CB2 receptor activation and the PPARγ pathway. *Pharmacology*, *94*(1-2), 1-12. https://doi.org/10.1159/000362689

Cushing, D., Goakar, D., Joseph, B. (2018). Differential calcification reduction of valvular interstitial cells by cannabidiol bioactivity and concentration. *Journal of Medical Phyto Research*, *2*(2), 14-22. https://doi.org/10.31013/2001f

Cushing, D., Kristipati, S., Shastri, R., & Joseph, B. (2018). Measuring the bioactivity of phytocannabinoid cannabidiol from cannabis sources, and a novel non-cannabis source. *Journal of Medical Phyto Research*, *10*.

de Simone, G., Izzo, R., Chinali, M., De Marco, M., Casalnuovo, G., Rozza, F., ... & De Luca, N. (2010). Does information on systolic and diastolic function improve prediction of a cardiovascular event by left ventricular hypertrophy in arterial hypertension?. *Hypertension*, *56*(1), 99-104. https://doi.org/10.1161/hypertensionaha.110.150128

Farrar, E. J., Pramil, V., Richards, J. M., Mosher, C. Z., & Butcher, J. T. (2016). Valve interstitial cell tensional homeostasis directs calcification and extracellular matrix remodeling processes via RhoA signaling. *Biomaterials*, *105*, 25-37. https://doi.org/10.1016/j.biomaterials.2016.07.034

Favata, M. F., Horiuchi, K. Y., Manos, E. J., Daulerio, A. J., Stradley, D. A., Feeser, W. S., ... & Copeland, R. A. (1998). Identification of a novel inhibitor of mitogen-activated protein kinase kinase. *Journal of Biological Chemistry*, *273*(29), 18623-18632. https://doi.org/10.1074/jbc.273.29.18623

Gerdts, E., Rossebø, A. B., Pedersen, T. R., Cioffi, G., Lønnebakken, M. T., Cramariuc, D., ... & Devereux, R. B. (2015). Relation of left ventricular mass to prognosis in initially asymptomatic mild to moderate aortic valve stenosis. *Circulation: Cardiovascular Imaging*, *8*(11), e003644. https://doi.org/10.1161/circimaging.115.003644

Gertsch, J., Leonti, M., Raduner, S., Racz, I., Chen, J. Z., Xie, X. Q., ... & Zimmer, A. (2008). Beta-caryophyllene is a dietary cannabinoid. *Proceedings of the National Academy of Sciences*, *105*(26), 9099-9104. https://doi.org/10.1211/jpp.59.12.0005

Gu, X., & Masters, K. S. (2009). Role of the MAPK/ERK pathway in valvular interstitial cell calcification. *American Journal of Physiology-Heart and Circulatory Physiology*, *296*(6), H1748-H1757. https://doi.org/10.1152/ajpheart.00099.2009

Hjortnaes, J., Shapero, K., Goettsch, C., Hutcheson, J. D., Keegan, J., Kluin, J., ... & Aikawa, E. (2015). Valvular interstitial cells suppress calcification of valvular endothelial cells. *Atherosclerosis*, *242*(1), 251-260. https://doi.org/10.1016/j.atherosclerosis.2015.07.008

Legault, J., & Pichette, A. (2007). Potentiating effect of β-caryophyllene on anticancer activity of α-humulene, isocaryophyllene and paclitaxel. *Journal of Pharmacy and Pharmacology*, *59*(12), 1643-1647. https://doi.org/10.1211/jpp.59.12.0005

Ligresti, A., De Petrocellis, L., & Di Marzo, V. (2016). From phytocannabinoids to cannabinoid receptors and endocannabinoids: pleiotropic physiological and pathological roles through complex pharmacology. Physiological reviews, 96(4), 1593- 1659. https://doi.org/10.1152/physrev.00002.2016

Mann, B. K., & West, J. L. (2002). Cell adhesion peptides alter smooth muscle cell adhesion, proliferation, migration, and matrix protein synthesis on modified surfaces and in polymer scaffolds. *Journal of biomedical materials research*, *60*(1), 86-93. https://doi.org/10.1002/jbm.10042

Michel, E. J. S., & Dipchand, A. I. (2017). Valvular Stenosis and Heart Failure. *Heart Failure in the Child and Young Adult: From Bench to Bedside*, 307. https://doi.org/10.1016/b978-0-12-802393-8.00023-5

Mohler III, E. R., Gannon, F., Reynolds, C., Zimmerman, R., Keane, M. G., & Kaplan, F. S. (2001). Bone formation and inflammation in cardiac valves. *Circulation*, *103*(11), 1522-1528. https://doi.org/10.1161/01.cir.103.11.1522

Poddighe, L., Carta, G., Serra, M. P., Melis, T., Boi, M., Lisai, S., ... & Quartu, M. (2018). Acute administration of beta-caryophyllene prevents endocannabinoid system activation during transient common carotid artery occlusion and reperfusion. *Lipids in health and disease*, *17*(1), 23. https://doi.org/10.1186/s12944-018-0661-4

Sharma, C., M Al Kaabi, J., M Nurulain, S., N Goyal, S., Amjad Kamal, M., & Ojha, S. (2016). Polypharmacological properties and therapeutic potential of β-caryophyllene: a dietary phytocannabinoid of pharmaceutical promise. *Current pharmaceutical design*, *22*(21), 3237-3264. https://doi.org/10.2174/1381612822666160311115226

Taylor, P. M., Batten, P., Brand, N. J., Thomas, P. S., & Yacoub, M. H. (2003). The cardiac valve interstitial cell. *The international journal of biochemistry & cell biology*, *35*(2), 113-118. https://doi.org/10.1016/s1357-2725(02)00100-0

Yoon, W. J., Moon, J. Y., Song, G., Lee, Y. K., Han, M. S., Lee, J. S., ... & Hyun, C. G. (2010). Artemisia fukudo essential oil attenuates LPS-induced inflammation by suppressing NF-κB and MAPK activation in RAW 264.7 macrophages. *Food and Chemical Toxicology*, *48*(5), 1222-1229. https://doi.org/10.1016/j.fct.2010.02.014

Zandbergen, F., & Plutzky, J. (2007). PPARα in atherosclerosis and inflammation. *Biochimica et Biophysica Acta (BBA)-Molecular and Cell Biology of Lipids*, *1771*(8), 972-982. https://doi.org/10.1016/j.bbalip.2007.04.021

Appendix:

	Treatment	5mg	10mg	25mg	40mg	100mg
1548	CBD	21.9	32.5	34.9	39.6	52.5
1730	CBD	19.2	18.5	27.7	43	43
1194	CBD	21.4	24.2	34	47.9	59.8
1785	CBD	21.2	27.9	29.2	42.6	55.6
1772	CBD	18.9	26.8	34.4	47.7	59
1169	CBD	19.7	24	30.3	46.8	50.7
1245	CBD	19.8	20.8	34.8	47.1	51.4
1496	CBD	19.4	31	31.6	44.8	41.9
1381	CBD	20.5	27.9	31.4	46.7	60.4
1380	CBD	16.7	25.4	42.4	36.5	62
1230	CBD	21.7	25.1	29.7	36.7	66.1
1655	CBD	18.8	27	42.6	43	59.6
1175	CBD	19.8	22.6	32.3	38.5	63.2
1617	CBD	17.6	28.1	35.6	51.1	51.5
1042	CBD	18.5	27.1	34.1	41.6	57

1640	CBD	18.8	22.3	31	46.1	64.7
1082	CBD	16.5	28.7	30.4	37.9	58.4
1743	CBD	18.5	24.3	29.7	36.9	56.7
1278	CBD	22.1	23.5	39.3	44.1	41.9
1134	CBD	20.4	25.7	34.3	42.1	51.9
1452	CBD	16.6	26.3	38.9	39.2	43.6
1696	CBD	19.7	24.8	28.6	35.8	56.6
1765	CBD	18.7	27.2	32.2	39.6	56.3
1032	CBD	21.1	27.4	31.9	38.9	59.3
1850	CBD	21.9	21.3	26.5	44.1	52
2018	CBD	15.4	25.6	28.6	47.6	53.6
1205	CBD	19.6	24.1	26.3	54.5	56.4
1548	ImmunAG	23.7	23.4	41.9	46.8	56.1
1730	ImmunAG	21.3	23	26.9	54.8	74.5
1194	ImmunAG	24.4	26.3	39.2	51.6	78.1
1785	ImmunAG	23.3	30.6	37.6	54.3	73.4
1772	ImmunAG	23.8	39.7	38.4	49.8	53.4
1169	ImmunAG	25	36.1	38.1	49.9	53.7
1245	ImmunAG	25.3	29.2	38.9	52.9	59.1
1496	ImmunAG	21.3	29.2	46.1	57	66.8
1381	ImmunAG	24.2	23.5	38.1	55.7	54.9
1380	ImmunAG	23.4	31.5	35.1	56.6	51.3
1230	ImmunAG	26.5	32.3	45.9	55.3	66.6
1655	ImmunAG	25.4	32	41.4	50.2	57.3
1175	ImmunAG	23.7	34.7	39.6	53.3	56.7
1617	ImmunAG	24.6	31.2	35.7	51.8	56.1
1042	ImmunAG	24.2	19	42.6	53	63.5
1640	ImmunAG	22.9	25.1	42.5	53.1	72.4
1082	ImmunAG	27.5	31.3	36.5	52	70
1743	ImmunAG	24.7	27.8	42.7	50.7	58.8
1278	ImmunAG	25.1	33.5	31.9	49.7	74.5
1134	ImmunAG	27.8	37.7	39.1	57.2	64.3
1452	ImmunAG	25.3	34.1	43.3	60	77.7
1696	ImmunAG	20.1	35.4	38.3	54.1	64.6
1765	ImmunAG	25.1	33	39.6	59.9	71.6
1032	ImmunAG	22.2	27.2	34.3	48	62.8
1850	ImmunAG	26.2	30	29.5	44.6	63.3
2018	ImmunAG	24.7	27.5	37.3	51.7	67.7
1205	ImmunAG	24.9	36.1	39.7	52.4	64.5

Citation: Cushing, C., Goakar, D., Joseph, B. (2018). Bioactive cannabidiol more greatly reduces valvular interstitial cell calcification when combined with ß-Caryophyllene, and α-Humulene. Journal of Medical Phyto Research, 2(2), 27-34. https://doi.org/10.31013/2001f

Recieved: August 25, 2018
Accepted: September 7, 2018
Published: September 26, 2018